

Induction of denitrification in a pilot-scale trickling filter by adding nitrate at high loading rate

H. Vanhooren*, D. De Pauw and P.A. Vanrolleghem

BIOMATH, Ghent University, Coupure Links 653, B-9000 Ghent, Belgium

(E-mail: *Peter.Vanrolleghem@rug.ac.be*)

* Currently: EPAS NV, Venecoweg 19, B-9810 Nazareth, Belgium (E-mail: *h.vanhooren@epas.be*)

Abstract Oxygen transferred from the liquid phase into a biofilm can be used for aerobic degradation of organic matter and for nitrification. A second possible pathway for the removal of organic matter is denitrification in anoxic zones deeper in the biofilm. At high organic loading rates with insufficient oxygen supply to the biofilm, denitrification could be induced by providing the biofilm with external nitrate. This possibility was tested in a pilot-scale trickling filter by adding a pulse of nitrate to a highly loaded trickling filter. The experiment showed that denitrification can indeed be induced by adding nitrate at high loading conditions and that this way a considerably increased substrate removal capacity can be obtained. The fact that denitrification occurred was confirmed by the increased production of CO₂ from bioconversion processes, without a major change of the O₂ consumption. The simplified mixed-culture biofilm model developed by Rauch *et al.* was extended for the description of off-gas measurements and was able to describe the results of the experiment very well.

Keywords Biofilm; denitrification; mass transfer; modelling and simulation; wastewater treatment

Introduction

Aerobic degradation in a trickling filter, or more generally in all biofilm systems, is mainly limited by the amount of oxygen that can be transferred from the liquid phase to the biofilm. In literature, it has been stated that the oxygen uptake of biofilms is on average 10 g O₂ m⁻²d⁻¹ (see among others: Logan, 1993; Hinton and Stensel, 1994). This oxygen can be used for aerobic degradation of organic matter, and, if any is left after this conversion process, nitrification can proceed. For the removal of organic matter a second pathway exists, i.e. denitrification in the anoxic zones of the biofilm. At high organic loading rates whenever the oxygen supply to the biofilm is insufficient, one can expect to induce/stimulate denitrification by providing the biofilm with additional nitrate. This possibility was tested in a pilot-scale trickling filter by adding a pulse of nitrate to a highly loaded trickling filter. The response was monitored using measurements in the liquid phase and in the off-gas of the filter system. The measured response was also modelled using a simplified mixed culture biofilm model (Rauch *et al.*, 1999; Vanhooren, 2001).

Pilot-scale trickling filter

The pilot-scale trickling filter that was used was constructed in order to evaluate non-invasive measurement techniques for use in calibration of models for process optimisation (Vanhooren *et al.*, 1999; Vanhooren, 2001). Among other measurements, the off-gas was continuously monitored for CO₂ and O₂. The filter unit's dimensions were chosen to represent a cylindrical core taken from a full-scale unit. The filter surface area $A = 0.118 \text{ m}^2$, and the volume $V = 0.213 \text{ m}^3$. To allow easy quantification of specific surface area and biofilm parameters, a plastic carrier medium (polypropylene) with specific surface area of 220 m²/m³ was chosen. An overview of the filter hydraulics can be seen on Figure 1. During normal operation, a synthetic influent (Boeije, 1999) is used. However, during the

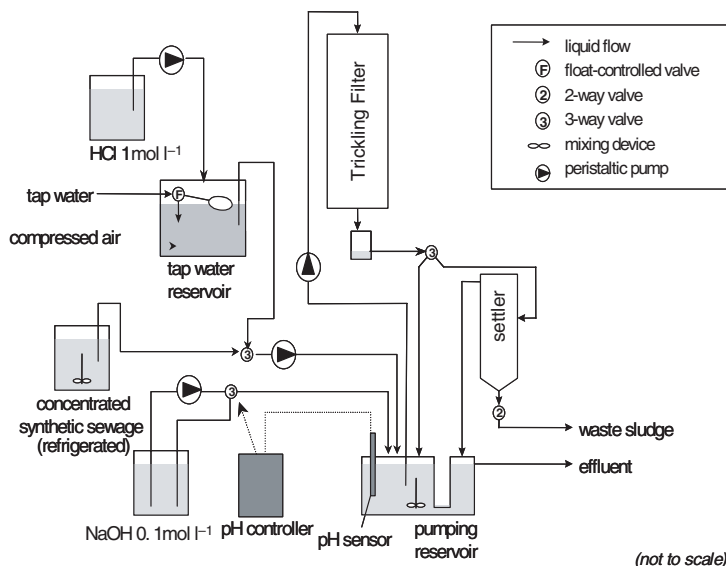


Figure 1 Overview of trickling filter hydraulics

time of this experiment, the carbon source used was ethanol. Also the settler was taken from the set-up to facilitate the hydrodynamic modelling of the filter. During the experiment, an airflow rate of 15 l/min was applied through the filter column. The influent flow rate was $0.418 \text{ m}^3/\text{d}$ and the applied recycle ratio was 3.5.

In the pumping tank, a pH control system was installed to adjust the pH to a value of 7.0. Only acidifying pH-control was foreseen. This control was needed since the influent was added at a pH as low as 4.5 to be able to remove most of the inorganic carbon in the tap water via stripping prior to its addition to the trickling filter.

Nitrate addition test

The test started with a period of low loading. The influent composition during this period is denoted in Table 2. After a small disturbance of the measurement system due to calibration of the pumps and the off-gas analysis equipment, the COD loading to the system was increased significantly while the nitrogen loading remained equal (Table 2). Measurements in Table 2 are averages over 4 measurements except for the nitrate concentration at high loading, for which only one measurement was available. In Figure 2 the off-gas concentrations of CO_2 and O_2 are depicted. From the O_2 leaving the filter (inlet concentration is 20.93 vol %) one can calculate the respiration rate, whereas the CO_2 concentration reflects the CO_2 that is transferred to the gas phase (inlet concentration is only 0.03 vol %). Note, however, that a considerable amount of biologically produced CO_2 leaves the reactor as accumulated bicarbonate via the effluent.

After about five hours, during which the system was allowed to stabilise in the high loading operation mode, dosing of extra nitrate to the influent was started. The influent nitrate concentration used was $83.5 \pm 0.5 \text{ mg N/l}$. The dosing of nitrate was continued for about 20 hours. Three hours before the end of this dosing, the pumps were calibrated, introducing a disturbance on the signal. Especially the CO_2 off-gas signal suffered from this disturbance, since the calibration includes the introduction of some fresh water into the set-up (Figure 2). This water did not necessarily have the same IC-concentration as the bulk liquid in the filter at that moment and can have had an effect on the pH in the trickling filter. Unfortunately, measurements of the pH in the pumping tank and in the filter's effluent were not stored during this period and this hypothesis can thus not be checked.

At the start of the nitrate dosing, an extra degradation of organic matter by denitrification was expected. This obviously did not cause a substantial change of the oxygen uptake in the filter, but it had an effect on the carbon dioxide production (Figure 2). This carbon dioxide was formed in the deeper, anoxic, layers of the biofilm.

It is important to note that a constant pH of 7.0 could be guaranteed by the pH control system during the complete period before the nitrate dosing experiment. However, pH values higher than 7.0 in the filter set-up were possible because acid addition to the pumping reservoir was not foreseen since this was not necessary during normal operation. During the nitrate dosing period, a considerable amount of alkalinity was produced by the denitrification process. This caused the pH to gradually increase up to a value of 7.29 in the effluent of the trickling filter. This makes clear that the amount of inorganic carbon stripped from the influent was high enough to seriously compromise the buffering capacity of the bulk liquid in the filter. Unlike the higher pH in the trickling filter effluent, the pH in the pumping tank was at most 7.15 due to the dosing of the low pH influent.

These pH measurement results were incorporated in the modelling of the nitrate dosing test. It should however be clear that the pH value is not an output of the modelling, but is considered as an input. This simplification has been made since pH electrodes are widespread in wastewater treatment and are known to be robust sensors. Complete modelling of the pH and the equilibria associated with it would substantially complicate the model and make it more vulnerable to numerical problems.

When the dosing of nitrate to the filter was stopped, the pH almost instantaneously decreased to its normal working value of 7.0. However, due to the high pH, quite some IC had accumulated in the bulk liquid of the filter in the form of HCO_3^- . When the pH dropped after stopping the nitrate addition, this extra IC was transferred to $\text{CO}_{2,\text{aq}}$ and was partly transferred to the gas phase. This gave rise to a clear “bump” in the CO_2 off-gas signal (Figure 2, phase 6).

After about 3 hours, the loading was lowered again, and a drop of the O_2 consumption and the CO_2 production could be seen.

Model description of the nitrate addition test

To model the load shift experiment, the simplified mixed culture biofilm model developed by Rauch *et al.* (1999) was used. This model had to be extended with a submodel for the description of the production and gas-liquid exchange of carbon dioxide. This submodel

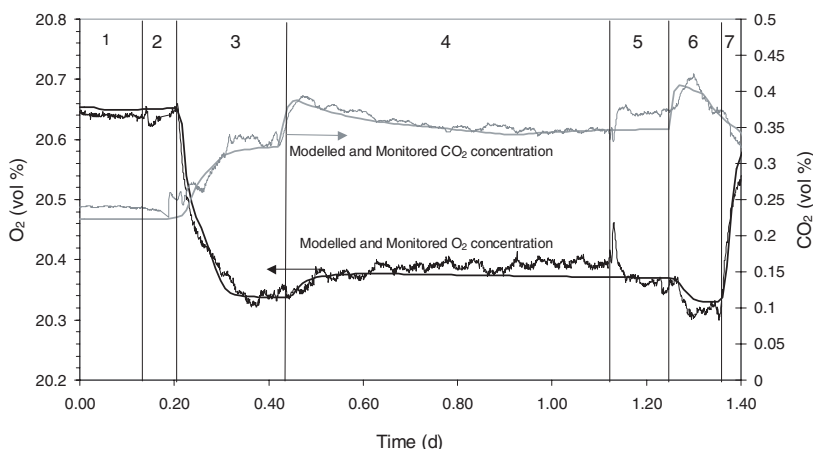


Figure 2 Monitored and modelled off-gas response to nitrate addition (numbers indicate phases given in Table 1)

Table 1 Overview of the trickling filter operation

Phase	Trickling filter operation
1	Low loading rate (C-source = ethanol)
2	Pump and off-gas equipment calibration
3	Increased loading rate
4	Nitrate addition to the filter
5	Pump calibration and cleaning of tubing
6	Stop of nitrate addition
7	Low loading rate

Table 2 Influent composition at low and high loading

Compound	Low loading	High loading
COD (mg/l)	134.5 ± 2.1	653.6 ± 28.4
NH ₄ ⁻ (mg N/l)	18.5 ± 0.42	15.45 ± 0.49
NO ₃ ⁺ (mg N/l)	4.29 ± 0.06	4.68

was based on the model developed by Spérandio and Paul (1997). In the extended model, the amount of CO₂ produced/used by the biomass can be written as the sum of the carbon dioxide produced during oxic and anoxic heterotrophic growth r_{H,CO_2} and the CO₂ used during nitrification, r_{A,CO_2} :

$$r_{CO_2} = r_{H,CO_2} - r_{A,CO_2} \quad \left[\frac{\text{g CO}_2}{\text{m}^3\text{d}} \right] \quad (1)$$

During heterotrophic growth, it is assumed that all organic carbon that is converted by the biomass is converted into either CO₂ or new cells. If the turnover of readily biodegradable COD is written as r_{S_S} , the production rate of biomass as r_{X_H} and the relation between the organic carbon and the COD in these species is denoted as i_C , we can write:

$$r_{H,C} = \left[r_{S_S} \cdot i_{C,S_S} \right] - \left[r_{X_H} \cdot i_{C,X_H} \right] \quad \left[\frac{\text{g TOC}}{\text{m}^3\text{d}} \right] \quad (2)$$

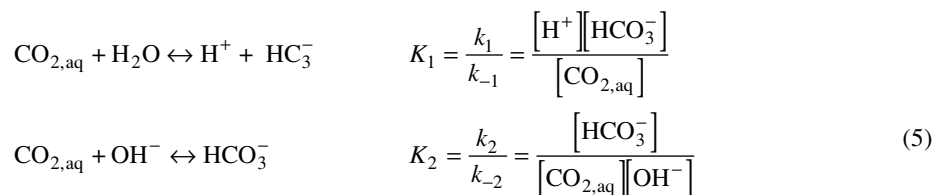
and for the production of carbon dioxide:

$$r_{H,CO_2} = r_{H,TOC} \cdot \frac{44}{12} \quad \left[\frac{\text{g CO}_2}{\text{m}^3\text{d}} \right] \quad (3)$$

On the other hand, the CO₂ uptake of the nitrifying biomass is proportional to the growth of autotrophic biomass.

$$r_{A,CO_2} = \left[r_{X_A} \cdot i_{C,X_A} \right] \cdot \frac{44}{12} \quad \left[\frac{\text{g CO}_2}{\text{m}^3\text{d}} \right] \quad (4)$$

Excess CO₂ is released to the liquid phase or, in case of net consumption, CO₂ is taken up from the liquid phase. In the liquid phase, the following equilibrium reactions with their corresponding dissociation constants K_1 and K_2 play an important role.



Note that the concentrations of the different components in the above equations are expressed in molar units. The production rate of bicarbonate can thus be written as

$$r_{\text{HCO}_3^-} = 44 \cdot \left(k_1 [\text{CO}_{2,\text{aq}}] - k_{-1} [\text{HCO}_3^-][\text{H}^+] + k_2 [\text{CO}_{2,\text{aq}}][\text{OH}^-] - k_{-2} [\text{HCO}_3^-] \right) \quad \left[\frac{\text{g CO}_2}{\text{m}^3\text{d}} \right] \quad (6)$$

The production of CO₂, combined with the equilibria described above, gives rise to the following mass balance equations:

$$\begin{aligned}
 V_L \frac{d[\text{CO}_{2,\text{aq}}]}{dt} &= \frac{r_{\text{CO}_2}}{44} V_L - \frac{r_{\text{HCO}_3^-}}{44} V_L - \phi_{\text{CO}_2}^{L \rightarrow G} + \phi_{\text{CO}_2}^L \\
 V_L \frac{d[\text{HCO}_3^-]}{dt} &= \frac{r_{\text{HCO}_3^-}}{44} V_L + \phi_{\text{HCO}_3^-}^L
 \end{aligned}
 \tag{7}$$

whereby V_L is the volume of the liquid phase, $\phi_{\text{CO}_2}^L$ and $\phi_{\text{HCO}_3^-}^L$ are the transport terms of CO₂ and HCO₃⁻ in the liquid phase. The mass transfer between gas and liquid phase for carbon dioxide is expressed as

$$\phi_{\text{CO}_2}^{L \rightarrow G} = \text{CTR} = K_L a^{\text{CO}_2} \cdot \left([\text{CO}_{2,\text{aq}}] - [\text{CO}_{2,\text{aq}}]^{\text{sat}} \right) \cdot V_L \quad \text{with} \quad [\text{CO}_{2,\text{aq}}]^{\text{sat}} = \frac{P_{\text{CO}_2}}{H_{\text{CO}_2}} \tag{8}$$

where P_{CO_2} is the partial pressure for CO₂ in the gas phase (atm) and H_{CO_2} is the Henry constant for CO₂ (atm⁻¹M).

This model was integrated in a hydrodynamic model based on the ‘‘Continuously Stirred Biofilm Reactor’’ approach (Wik and Breitholz, 1996). Each CSBR consists of a CSTR connected to a biofilm compartment by a diffusive link. Based on the results of a tracer test (Vanhooren *et al.*, 1999; Vanhooren, 2001), 7 CSBRs in series were used. In Table 3 the parameter set used for the model description of the experiment is given. For the correct description of the off-gas measurement results, the actual value of the TOC/COD ratio of ethanol was implemented. This is 0.25 g TOC/g COD.

In this experiment, the diffusion coefficient for readily biodegradable substrate appears to govern the amount of denitrification that proceeds after the nitrate addition. At the start of the calibration process, a diffusion coefficient of 0.58 cm²/d was used for the readily biodegradable substrate S_S , which is the default value in the model. With this value a discrepancy between the measured and predicted O₂ concentration was seen in the period with nitrate addition. This was probably the result of a very high denitrification activity predicted by the model at the top of the filter. There, the readily biodegradable ethanol diffused relatively deep into the biofilm. This meant that the readily biodegradable substrate was simulated to be depleted by the time the water reached the bottom of the filter. Consequently, limitation of readily biodegradable substrate started to prevail in the lower sections of the filter. This increased denitrification leads in its turn to a decreased use of oxygen as a smaller fraction of the supplied readily biodegradable substrate is aerobically degraded, leaving part of the aerobic degradation capacity of the filter unused.

However, it is very unlikely that this phenomenon happened to this extent in reality, especially because the effluent concentration of soluble COD was measured to be over

Table 3 Biodegradation model parameters ([a] Spérandio and Paul (1997))

CO ₂ /HCO ₃ ⁻ equilibrium and mass transfer parameters			Biofilm characteristics		
k_1	0.018 [a]	s ⁻¹	μ_H [growth rate heterotrophs]	4	d ⁻¹
K_1	4.065×10^{-7} [a]	mol.L ⁻¹	Y_H [heterotrophic yield]	0.6	g COD/g COD
k_2	4600 [a]	L.(mol/s) ⁻¹	b_H [heterotrophic decay]	0.4	d ⁻¹
K_2	$4.065 \times 10^{+7}$ [a]	L.mol ⁻¹	k_r [hydrolysis of S_R]	50	d ⁻¹
$K_{L,a}(\text{O}_2)$	2400	d ⁻¹	k_r [hydrolysis of X_S]	5	d ⁻¹
$K_{L,a}(\text{CO}_2)$	2160	d ⁻¹	k_a [ammonification of S_{ND}]	0.1	m ³ .(g COD/d) ⁻¹
$D_i(\text{O}_2)$	2.1×10^{-5}	cm ² /s	k_{at} [attachment coefficient]	4	d ⁻¹
$D_i(S_S)$	0.28×10^{-5}	cm ² /s	k_{dt} [detachment coefficient]	0.05	d ⁻¹
$D_i(S_{NO})$	1×10^{-5}	cm ² /s	ρ_m [biomass density]	38.8	kg.m ⁻³

30 mg/l during the nitrate addition, indicating remaining ethanol. Moreover, the model overestimated the nitrate consumption. An effluent concentration as high as 40 mg NO_3^- -N/l was measured during the addition period (Figure 3). Although the number of off-line measurements during the test was rather limited, the trend is clear in these figures.

Based on the above findings, the diffusion coefficient for the readily biodegradable substrate S_5 was changed and by manual tuning via trial and error a value of $0.28 \text{ cm}^2/\text{d}$ was selected. The result can be seen in Figure 2. It is clear that the increase of the oxygen concentration due to substrate limitation in the lower section of the trickling filter is very small with this diffusion coefficient. Also, the agreement with the off-line measurements is good (Figure 3), although the effluent substrate concentration at high loading rate without nitrate addition is somewhat underestimated.

In Figure 4 the dimensionless penetration depths of the substrates in the biofilm are depicted. These depths correspond to the fraction of the biofilm that is penetrated by the considered substrate. At low loading, substrate is limiting all conversion processes. At high loading, oxygen took over this role. Only a very limited amount of denitrification was present as can be concluded from the almost overlapping aerobic and anoxic growth penetration depths. When nitrate was added, oxygen still limited aerobic metabolism, but more substrate could be degraded via denitrification as seen from the considerably deeper penetration depth for anoxic activity. This situation was reversed again when the nitrate dosing was stopped and further when the loading was lowered.

The overall model description of the experiment is very good (Figure 2). During the phases 1 until 3, a constant pH value of 7.05 was used in the simulations. During the nitrate

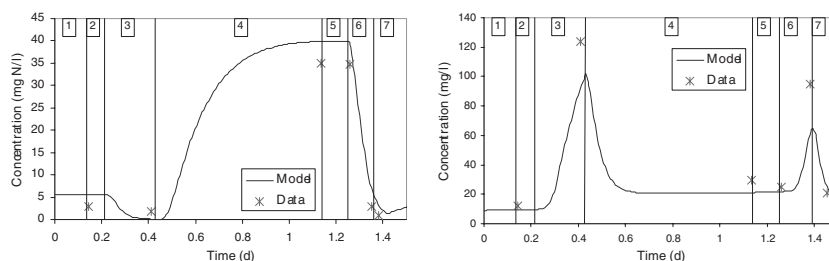


Figure 3 Measured and simulated nitrate (left) and readily biodegradable COD (right) concentration during the nitrate addition test ($D_{f,S_5} = 0.28 \text{ cm}^2/\text{d}$) (numbers indicate phases given in Table 1)

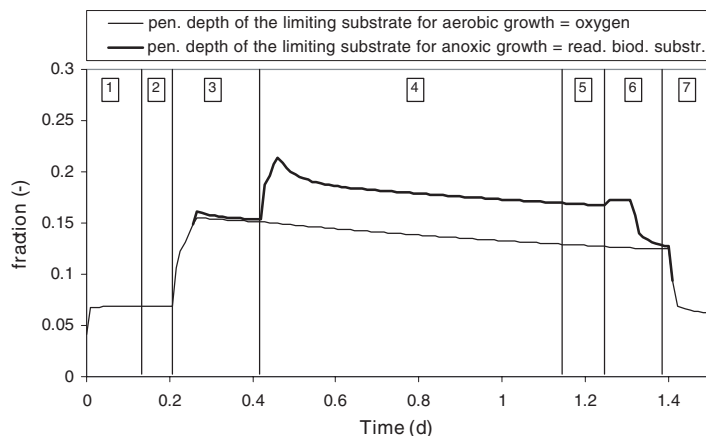


Figure 4 Dimensionless penetration depths of the substrates limiting aerobic and anoxic growth in the middle of the filter set-up (numbers indicate phases given in Table 1)

addition, the gradual pH-increase up to 7.26 in the filter's effluent was implemented. This increase decreased the CO₂ transfer to the gas phase and explains the declining CO₂ concentration in the gas phase along phase 4. In phase 6, the extra IC accumulated in the liquid phase was stripped to the gas phase when the pH in the filter dropped down to 6.83.

Increased conversion capacity

As described above, stimulation of denitrification could be interesting to overcome periods where the treatment capacity of a biofilm system is insufficient. At high organic loading rates, and whenever oxygen supply is insufficient to obtain good treatment capacity, denitrification could be induced by providing the biofilm with another electron acceptor besides oxygen. As Figure 4 shows, the effluent COD concentration increased quite drastically with the higher load to the filter. However, the filter didn't have the time to stabilise completely before nitrate addition was started. It is therefore difficult to assess the extra treatment capacity obtained by denitrification from the experimental results.

Using the model, however, estimates of the extra capacity of the filter can be made. It turns out that 54.3 g COD/d were removed using the denitrification pathway on top of the 206.1 g COD/d removed via aerobic degradation. For this extra COD removal capacity, 22.0 g NO₃⁻-N g/d was used. Using the effluent quality calculation proposed in the COST simulation benchmark (Copp, 2001) and the cost multiplication factors proposed by Vanrolleghem and Gillot (2002), the effluent fine for COD is estimated to be € 0.137 /kg COD. The cost for industrial application of nitrate-nitrogen is estimated to be about € 0.7 /kg NO₃⁻-N. Consequently, at first sight, the addition of nitrate is not an economically feasible solution. However, the effluent fines for COD are highly country-specific and are subject to rises in the future. Moreover, no extra penalty for the violation of effluent constraints is included in these numbers. On the other hand, in many industries, cheap nitrate sources are available as a waste product. This nitrate could be used to perform denitrification as proposed here.

Conclusions

This experiment shows that denitrification can indeed be induced by adding nitrate at high loading conditions and that this way a considerably increased substrate removal capacity can be obtained. The production of CO₂ from bioconversion processes increased, while no major change of the O₂ consumption was noticed. The simplified mixed-culture biofilm model extended for the description of off-gas measurements was able to describe the results of the experiment very well.

Acknowledgement

Financial support for this work was provided by the Fund for Scientific Research – Flanders (Belgium) (F.W.O.). The first author is Research Assistant of the Fund for Scientific Research – Flanders (Belgium).

References

- Boeije, G.M. (1999). *Chemical fate prediction for use in geo-referenced environmental exposure assessment*. PhD Thesis, Faculty of Agricultural and Applied Biological Sciences, Ghent University, Ghent.
- Copp, J.B. (2001). *The COST Simulation Benchmark: Description and Simulator Manual*. Office for Official Publications of the European Community, Luxembourg.
- Hinton, S.W. and Stensel, H.D. (1994). Oxygen utilization of trickling filter biofilms. *J. Environ. Eng.*, **120**, 1284–1297.
- Logan, B.E. (1993). Oxygen transfer in trickling filters. *J. Environ. Eng.*, **119**, 1059–1076.
- Rauch, W., Vanhooren, H. and Vanrolleghem, P.A. (1999). A simplified mixed-culture biofilm model. *Wat. Res.*, **33**, 2148–2162.

- Spérandio, M. and Paul, E. (1997). Determination of carbon dioxide evolution rate using on-line gas analysis during dynamic biodegradation experiments. *Biotechnol. Bioeng.*, **53**, 243–252.
- Vanhooren, H. (2001). *Modelling for optimisation of biofilm wastewater treatment processes: a complexity compromise*. PhD Thesis, Faculty of Agricultural and Applied Biological Sciences, Ghent University, Ghent.
- Vanhooren, H., Boeije, G., Accoe, F. and Vanrolleghem, P.A. (1999). Non-invasive and continuous monitoring of a pilot-scale trickling filter: weight, off-gas and hydraulic characterization. In: *Preprint IAWQ Conference on Biofilm Systems*, New York, October 17–20, 1999.
- Vanrolleghem, P.A. and Gillot, S. (2002). Robustness and economic measured as control benchmark performance criteria. *Wat. Sci. Tech.*, **45**(4–5), 117–126.
- Wik, T. and Breitholz, C. (1996). Steady state solution of a two-species biofilm problem. *Biotechnol. Bioeng.*, **50**, 675–686.